

ORIGINAL ARTICLE

Cloud points in aqueous solutions of poly(*N*-isopropylacrylamide) synthesized by aqueous redox polymerization

Tomoyo Ise, Kouta Nagaoka, Masashi Osa and Takenao Yoshizaki

The mean-square radius of gyration, second virial coefficient and intrinsic viscosity were determined in methanol at 25.0 °C for poly(*N*-isopropylacrylamide) (PNIPA) samples in the range of weight-average molecular weight M_w from 1.04×10^5 to 2.65×10^6 , which were synthesized by aqueous redox polymerization using a redox catalyst consisting of ammonium persulfate and sodium metabisulfite. Analyses of the quantities showed that the samples have almost the same degree of branching as that of PNIPA samples previously synthesized by radical polymerization using azobis(isobutyronitrile) as an initiator in *tert*-butanol. The cloud point was also determined in aqueous solutions of two PNIPA samples with $M_w = 1.04 \times 10^5$ and 1.86×10^5 and compared with the results of the previous samples. It was found that the cloud point is definitely higher for the present samples than for the previous ones, and, moreover, the M_w dependences of the cloud point for the two kinds of samples are opposite to each other. As the two kinds of samples have almost the same stereochemical composition and degree of branching, such difference in the behavior of the cloud point is considered to arise from the difference in their chain-end groups.

Polymer Journal (2011) 43, 164–170; doi:10.1038/pj.2010.121; published online 15 December 2010

Keywords: aqueous solution; cloud point; intrinsic viscosity; mean-square radius of gyration; poly(*N*-isopropylacrylamide); second virial coefficient

INTRODUCTION

In a series of experimental studies recently made of aqueous poly(*N*-isopropylacrylamide) (PNIPA) solutions,^{1–4} it was shown that the behavior of their cloud-point curves is considerably affected by the kind of end group of the PNIPA sample used^{1,3} and also by primary structure, that is, the degree of branching of the sample.² Furthermore, it was pointed out that the cloud-point curve does not seem to correspond directly to a liquid–liquid binodal.⁴

The PNIPA samples used previously^{1–4} were synthesized by radical polymerization using azobis(isobutyronitrile) (AIBN) as an initiator and by living anionic polymerization using diphenylmethylpotassium as an initiator, so that they had hydrophobic groups at their chain ends, that is, the isobutyronitrile group for the former and the diphenylmethyl group for the latter. The above-mentioned aqueous solution behavior of PNIPA may arise from the effect of the hydrophobic chain-end groups, which is enhanced with decreasing molecular weight. To verify more clearly the effect of the chain-end groups on the behavior of the cloud-point curve, it is desirable to pursue further investigations of aqueous solution behavior of PNIPA samples with a hydrophilic chain-end groups.

In this study, therefore, we prepared such PNIPA samples by aqueous redox polymerization using a redox catalyst consisting of ammonium persulfate and sodium metabisulfite, whose chain-end

groups are hydrophilic and/or ionic ones. We first characterized the PNIPA samples so prepared by analyzing dilute solution properties such as the mean-square radius of gyration $\langle S^2 \rangle$, second virial coefficient A_2 and intrinsic viscosity $[\eta]$, in methanol at 25.0 °C, then determined the cloud point in the aqueous solutions, and finally made a comparison of present results with the previous ones for the PNIPA samples having the hydrophobic chain-end groups.¹

EXPERIMENTAL PROCEDURE

Materials

Original PNIPA samples were synthesized by aqueous redox polymerization using a redox catalyst consisting of ammonium persulfate ($(\text{NH}_4)_2\text{S}_2\text{O}_8$ (Wako Pure Chemical Industries, Ltd, Osaka, Japan) as an oxidative reagent and sodium metabisulfite $\text{Na}_2\text{S}_2\text{O}_5$ (Wako Pure Chemical Industries, Ltd) as a reductive reagent, following the procedure reported by Wooten *et al.*⁵ The monomer *N*-isopropylacrylamide (Tokyo Chemical Industry Co., Ltd, Tokyo, Japan; ~20 g), which had been recrystallized three times from a 9:1 mixture of *n*-hexane and benzene and then dried in a vacuum for 12 h, was dissolved in 250 ml of phosphate-buffered saline (PBS) with pH=7.3–7.5 (Lonza Walkersville, Inc., Walkersville, MD, USA). Subsequently, 0.09 g of $\text{Na}_2\text{S}_2\text{O}_5$ in 1 ml of PBS was added to the monomer solution, followed by 0.03 g of $(\text{NH}_4)_2\text{S}_2\text{O}_8$ in 1 ml of PBS. The reaction mixture was then stirred under dry nitrogen at 25 °C for 24 h. Then, the polymerization mixture was poured into 250 ml of methanol, to precipitate an original polymer sample.⁶ The resulting polymer

was then dissolved in pure water and dialyzed seven times against pure water for 24 h using a cellulose tube.

The original samples so prepared were separated into fractions of narrow molecular weight distribution by fractional precipitation using acetone as a solvent and *n*-hexane as a precipitant, or by a column elution method with a 6:4 mixture of *n*-hexane and acetone as an eluent. We obtained nine test samples named Rx ($x=10, 19, 21, 48, 66, 96, 130, 220$ and 270), which are generally called R samples. Each of the samples was dissolved in 1,4-dioxane, then filtered through a Teflon membrane Fluoropore (Sumitomo Electric Industries, Ltd, Osaka, Japan) with a pore size of $1.0\ \mu\text{m}$, and finally freeze-dried from their 1,4-dioxane solutions. They were dried in a vacuum at $\sim 80\ ^\circ\text{C}$ for 12 h just before use. The ratio M_w/M_n of the weight-average molecular weight M_w to the number-average molecular weight M_n was determined for the 9 samples from analytical gel permeation chromatography in the same manner as before^{1,3} using tetrahydrofuran as an eluent and 12 standard polystyrene (PS) samples as reference standards.

To specify the chain-end group of the present PNIPA samples, we synthesized an extra PNIPA sample with a very small M_w by mixing 10 g of *N*-isopropylacrylamide in 250 ml of PBS with 1.50 g of $\text{Na}_2\text{S}_2\text{O}_5$ in 25 ml of PBS and 0.50 g of $(\text{NH}_4)_2\text{S}_2\text{O}_8$ in 25 ml of PBS, in the same manner as above. The reaction mixture was stirred under dry nitrogen at $25\ ^\circ\text{C}$ for 30 min. The resulting polymer was dialyzed and then dried in the above-mentioned manner. The extra sample was named R0.5, whose values of M_w , M_n and M_w/M_n were determined to be 4.77×10^3 , 3.34×10^3 and 1.43, respectively, from analytical gel permeation chromatography with a column Shodex SB-804 HQ (Showa Denko KK, Tokyo, Japan) connected to a solvent delivery pump PU-980 (JASCO Corporation, Tokyo, Japan) and a refractive index detector RI-8000 (Tosoh Corporation, Tokyo, Japan); a 0.2 M aqueous NaNO_3 solution was used as an eluent and nine standard poly(oxyethylene) samples as reference standards.

Tetrahydrofuran used in analytical gel permeation chromatography was of reagent grade with no stabilizer. Deuterated dimethyl sulfoxide used for ^1H - and ^{13}C -nuclear magnetic resonance (NMR) spectroscopy was of reagent grade. Methanol used for static light scattering (LS) and viscosity measurements was purified by distillation after refluxing over calcium hydride for ~ 6 h. Water used for the determinations of the cloud point was highly purified through a water purification system Simpli Lab (Millipore Corporate, Billerica, MA, USA); its resistivity was $18.2\ \text{M}\Omega\ \text{cm}$.

^1H - and ^{13}C -NMR

To determine the values of the fraction f_i of racemo diads for all the nine samples, R10 through R270, ^1H NMR spectra for the samples in deuterated dimethyl sulfoxide at $170\ ^\circ\text{C}$ at $\sim 1\ \text{wt}\%$ were recorded on a spectrometer EX-400 (JEOL Ltd, Tokyo, Japan) at 399.8 MHz using an rf pulse angle of 90° and a pulse repetition time of 8 s. To specify the chain-end group of the present PNIPA samples, the ^{13}C NMR spectrum of the extra sample R0.5 in deuterated dimethyl sulfoxide at $150\ ^\circ\text{C}$ at $\sim 20\ \text{wt}\%$ was recorded on the same spectrometer, operated at 100.5 MHz with a pulse repetition time of 3 s. Tetramethylsilane was added to each solution as an internal standard.

Light scattering

LS measurements were carried out to determine M_w and A_2 for all nine samples, R10 through R270, and $\langle S^2 \rangle$ for the eight samples, R19 through R270, in methanol at $25.0\ ^\circ\text{C}$. A light-scattering photometer Fica 50 (Fica, Saint Denis, France) was used for all measurements with vertically polarized incident light of wavelength $\lambda_0=436\ \text{nm}$. To calibrate the apparatus, the intensity of the light scattered from pure benzene was measured at $25.0\ ^\circ\text{C}$ at a scattering angle of 90° , where the Rayleigh ratio $R_{\text{U}}(90^\circ)$ of pure benzene was taken as $46.5 \times 10^{-6}\ \text{cm}^{-1}$.⁷ The depolarization ratio ρ_{u} of pure benzene at $25.0\ ^\circ\text{C}$ was determined to be 0.41 ± 0.01 . The scattered intensity was measured at eight different concentrations and at scattering angles ranging from 22.5 to 142.5° , and then converted to the excess unpolarized components ΔR_{UV} of the reduced scattered intensity using the scattered intensity from the solvent methanol. The data obtained were treated by using the Berry square-root plot.⁸ For all samples, corrections for the optical anisotropy were unnecessary as the degree of depolarization was negligibly small.

The most concentrated solution of each sample was prepared gravimetrically and made homogeneous by continuous stirring at room temperature for 1 or 2 days. It was optically purified by filtration through a Teflon membrane Fluoropore with a pore size of 0.45 or $0.10\ \mu\text{m}$. The solutions of lower concentration were obtained by successive dilution. The weight concentrations of the test solutions were converted to polymer mass concentrations c using the densities of the respective solutions calculated from the partial specific volumes v_2 of the samples and the density ρ_0 of the solvent methanol. The quantity v_2 was measured using an oscillating U-tube density meter DMA5000 (Anton-Paar, Graz, Austria). The values of v_2 so determined in methanol at $25.0\ ^\circ\text{C}$ were 0.86_9 , 0.87_6 , 0.87_8 and $0.88_3\ \text{cm}^3\ \text{g}^{-1}$ for the samples R10, R19, R21 and R48, respectively, and $0.88_4\ \text{cm}^3\ \text{g}^{-1}$ for the samples with $M_w \geq 6 \times 10^5$, independent of M_w . For ρ_0 of methanol at $25.0\ ^\circ\text{C}$, we used the literature value $0.7866\ \text{g}\ \text{cm}^{-3}$.⁹

The refractive index increment $\partial n/\partial c$ was measured at a wavelength of $436\ \text{nm}$ using a differential refractometer DR-1 (Shimadzu Corporation, Kyoto, Japan). The values of $\partial n/\partial c$ in methanol at $25.0\ ^\circ\text{C}$ were determined to be 0.186_5 , 0.186_4 , 0.185_5 and $0.184_6\ \text{cm}^3\ \text{g}^{-1}$ for samples R10, R19, R21 and R48, respectively, and $0.185_1\ \text{cm}^3\ \text{g}^{-1}$ for samples with $M_w \geq 6 \times 10^5$, independent of M_w . For the refractive index n_0 of methanol at $25.0\ ^\circ\text{C}$ at a wavelength of $436\ \text{nm}$, we used the literature value 1.3337 .⁹

Viscosity

Viscosity measurements were carried out for all nine samples, R10 through R270, in methanol at $25.0\ ^\circ\text{C}$ using a conventional capillary viscometer of the Ubbelohde type. The flow time was measured to a precision of $0.1\ \text{s}$, keeping the difference in the flow time between the solvent and solution longer than $20\ \text{s}$. The test solutions were maintained at $25.0\ ^\circ\text{C}$ within $\pm 0.005\ ^\circ\text{C}$, during the measurements.

The most concentrated solution of each sample was prepared in the same manner as in the case of the LS measurements. The solutions of lower concentration were obtained by successive dilution. The polymer mass concentrations c were calculated from the weight fractions and the densities of the solutions. Density corrections were also made in the calculations of the relative viscosity η_r from the flow times of the solution and solvent. The data obtained for the specific viscosity η_{sp} and η_r in the range of $\eta_r < 1.8$ were treated, as usual, by the Huggins (η_{sp}/c vs c) and Fuoss–Mead ($\ln \eta_r/c$ vs c) plots, respectively, to determine $[\eta]$ and the Huggins coefficient k' . (Note that the two plots have the same intercept.)

Transmittance of light

The intensity of light passing through aqueous solutions of the samples R10 and R19 at various weight fractions w was measured using a home-made apparatus with incident light of wavelength $650\ \text{nm}$ from a laser diode module. A given test solution contained in a cylindrical cell of outer diameter $10\ \text{mm}$ was immersed in a water bath and stirred continuously. The temperature of the water bath was made to increase at a rate of $\sim 1.5\ ^\circ\text{C}\ \text{h}^{-1}$. During the continuous increase in temperature from 30 to $35\ ^\circ\text{C}$, the intensity of the light passing through the cell was monitored by a photodiode. The output of the photodiode and the solution temperature, measured simultaneously using a platinum resistance thermometer combined with a programmable digital multimeter 7555 (Yokogawa Electric Corporation, Tokyo, Japan), were recorded on a personal computer at intervals of $10\ \text{s}$. Then, the (relative) transmittance, as defined as the ratio of the intensity of light through the test solution at a given temperature to the intensity at a lower temperature at which the test solution is apparently transparent, was determined as a function of temperature.

The measurements were carried out for each sample at eight concentrations in the range of $0.5\% \leq w \leq 10\%$. The most concentrated solution of each sample was prepared gravimetrically and made homogeneous by continuous stirring for 2 days at $\sim 5\ ^\circ\text{C}$. The solutions of lower concentration were obtained by successive dilution.

RESULTS AND DISCUSSION

Characterization

Stereochemical compositions and chain-end groups. As shown in the second column of Table 1, the values of the fraction f_i of the racemo

Table 1 Values of f_r and M_w/M_n and results of LS and viscosity measurements for poly(*N*-isopropylacrylamide) in methanol at 25.0 °C

Sample	f_r	M_w	M_w/M_n^a	$10^{-4} \langle S^2 \rangle$ (Å ²)	$10^4 A_2$ (cm ³ mol g ⁻²)	Ψ	$[\eta]$ (100 ml per g)	k'	$10^{-23} \Phi$ (mol ⁻¹)
R10	0.54	1.04×10^5	1.61	—	4.8 ₇	—	0.575	0.36	—
R19	0.54	1.86×10^5	1.33	2.8 ₇	4.8 ₃	0.25 ₇	0.856	0.35	2.2 ₃
R21	0.53	2.14×10^5	1.27	3.3 ₀	4.3 ₆	0.24 ₈	0.980	0.36	2.3 ₈
R48	0.54	4.76×10^5	1.29	8.6 ₅	3.3 ₉	0.22 ₅	1.56	0.33	1.9 ₉
R66	0.54	6.59×10^5	1.25	12.6	3.3 ₄	0.24 ₀	2.03	0.33	2.0 ₂
R96	0.53	9.61×10^5	1.28	18.8	2.8 ₉	0.24 ₅	2.60	0.32	2.0 ₉
R130	0.54	1.34×10^6	1.26	25.7	2.7 ₀	0.27 ₇	3.18	0.33	2.2 ₂
R220	0.54	2.23×10^6	1.26	41.4	2.4 ₄	0.34 ₀	4.09	0.34	2.3 ₃
R270	0.53	2.65×10^6	1.27	45.4	2.0 ₉	0.35 ₇	4.79	0.34	2.8 ₂

Abbreviations: GPC, gel permeation chromatography; LS, light scattering; PS, polystyrene.

^aThe values of M_w/M_n were determined from analytical GPC using standard PS samples as reference standards.

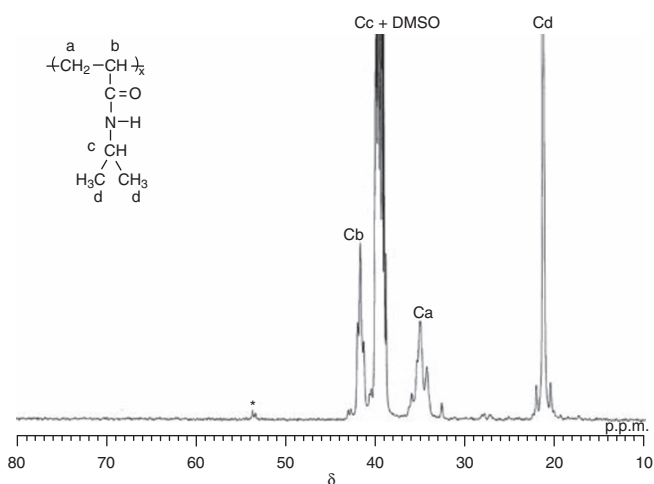


Figure 1 ¹³C nuclear magnetic resonance spectrum for the poly(*N*-isopropylacrylamide) sample R0.5 in the range of $10 \leq \delta/\text{p.p.m.} \leq 80$. The signal with the asterisk is from the methylene carbon adjacent to the initiating chain-end group. DMSO, dimethyl sulfoxide.

diads determined for all nine samples, R10 through R270, from ¹H NMR spectra using the assignments of the ¹H signals as proposed by Isobe *et al.*,¹⁰ are almost the same (0.53–0.54) and rather in good agreement with the f_r values (0.51–0.52) determined previously for the samples synthesized by radical polymerization using AIBN as an initiator in *tert*-butanol and benzene,¹ which are hereafter called T and B samples, respectively.

Figure 1 shows the ¹³C NMR spectrum of the extra sample R0.5 in the range of the chemical shift δ from 10 to 80 p.p.m., where signals from the methylene carbon C_a ($34 \leq \delta/\text{p.p.m.} \leq 36$)¹¹ and the methine carbon C_b ($41 \leq \delta/\text{p.p.m.} \leq 42$)¹¹ in the main chain, the methine carbon C_c ($38 \leq \delta/\text{p.p.m.} \leq 40$)¹¹ and the methyl carbon C_d ($20 \leq \delta/\text{p.p.m.} \leq 22$)¹¹ in the side group, and the carbons in the solvent dimethyl sulfoxide ($38 \leq \delta/\text{p.p.m.} \leq 40$) are observed. We note that a signal from the carbonyl carbon ($172 \leq \delta/\text{p.p.m.} \leq 174$)¹¹ is out of the range.

The small signal with the asterisk observed at $\delta \approx 54$ p.p.m. may arise from methylene carbons adjacent to the initiating chain-end groups. Analogous to polymers synthesized by aqueous redox polymerization using (NH₄)₂S₂O₈ and Na₂S₂O₅,^{12,13} the initiating chain-end of sample R0.5 may probably be sulfonate, sulfate or hydroxy groups, as shown in Figure 2. According to the report by Ebdon

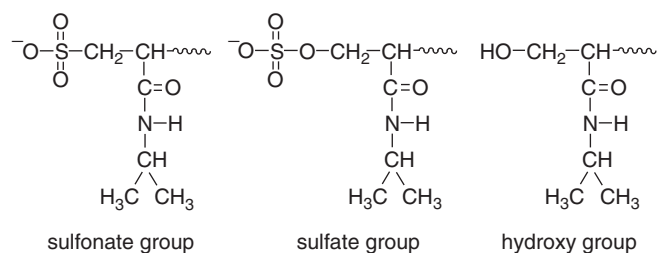


Figure 2 Chemical structures of probable initiating chain-end groups: sulfonate, sulfate and hydroxy groups.

et al.,¹² which stated that the signals from the methylene carbons adjacent to the sulfonate, sulfate and hydroxy groups at the initiating end of a vinyl polymer appear at $51 \leq \delta/\text{p.p.m.} \leq 52$, $61 \leq \delta/\text{p.p.m.} \leq 62$ and $64 \leq \delta/\text{p.p.m.} \leq 65$, respectively, the signal with the asterisk in Figure 1 may be assigned to the methylene carbon adjacent to the sulfonate end-group. As signals from the methylene carbons adjacent to the sulfate and hydroxy end groups are inappreciable in Figure 1, it may be concluded that almost all of the initiating chain-ends in the sample R0.5 are sulfonate groups. Although we could not directly specify the type of the initiating chain-end group for the nine samples, R10 through R270, because of the weakness of the signal from the methylene carbon adjacent to the initiating chain-end group, the sulfonate group may also be predominant in the samples synthesized in the same manner as was sample R0.5. As for the terminating end group of the present PNIPA samples, we do not have any detailed information.

Mean-square radius of gyration in methanol at 25 °C. The values of M_w and M_w/M_n determined from LS measurements in methanol at 25.0 °C and analytical gel permeation chromatography, respectively, for all nine samples, R10 through R270, are given in the third and fourth columns, respectively, of Table 1. The fifth column of the table gives the values of $\langle S^2 \rangle$ for the eight samples R19 through R270 determined simultaneously from the LS measurements in methanol at 25.0 °C. We note that the value of $\langle S^2 \rangle$ for sample R10 has been omitted because the slope of the Berry square-root plot against the square of the magnitude of the scattering vector was not sufficiently large for R10 to evaluate $\langle S^2 \rangle$ accurately.

Figure 3 shows double-logarithmic plots of $\langle S^2 \rangle$ (in Å²) against M_w ; the unfilled circles represent the present values for the R samples, and the solid curve smoothly connects the data points. For comparison, plots for the T and B samples have been reproduced from

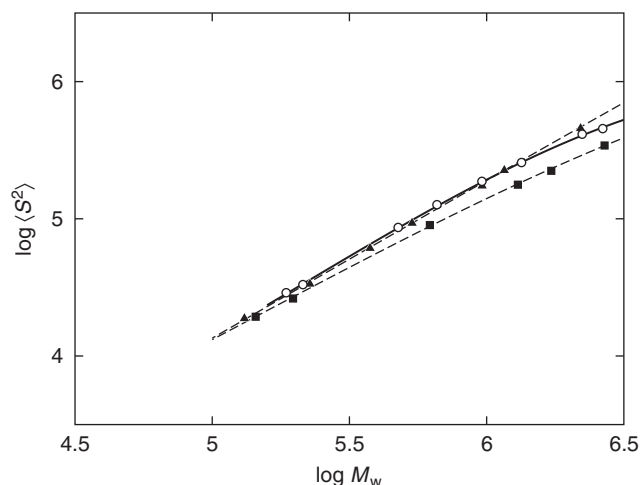


Figure 3 Double-logarithmic plots of $\langle S^2 \rangle$ (in \AA^2) against M_w for poly(*N*-isopropylacrylamide) in methanol at 25.0 °C: (○), R samples; (▲), T samples;² (■), B samples.² The curves smoothly connect the respective data points.

Figure 1 of ref. 2. The filled triangles and squares represent the values for the T and B samples, respectively, and dashed curves smoothly connect the respective data points.

The slope of the plot of the R samples in the range of $M_w \geq 10^6$ is 0.9₄ and intermediate between 1.1₂ and 0.9₀ for the T and B samples, respectively. The slope 0.9₄ is less than 1.2, which corresponds to linear flexible polymers with very large M_w in good solvents, and smaller than unity, which corresponds to unperturbed linear polymers. This implies that the primary structure of the R samples is not linear but branched, as in the cases of the T and B samples.² The values of $\langle S^2 \rangle$ for the R samples are in rather good agreement with the values for the T samples, but definitely larger than the values for the B samples. For a given polymer chain, $\langle S^2 \rangle$ generally decreases with the increasing degree of branching.¹⁴ Considering the fact that the R, T and B samples have almost the same stereochemical composition, therefore, the degrees of branching of the R and T samples agree with each other and are smaller than that of the B samples. Strictly, however, the data points for the R samples deviate downward from the point for the T samples for $M_w \geq 2 \times 10^6$. This implies that the degree of branching is somewhat larger for the R samples than for the T samples in the range of very large M_w .

Second virial coefficient in methanol at 25.0 °C. The values of A_2 determined from LS measurements in methanol at 25.0 °C for all nine samples, R10 through R270, are given in the sixth column of Table 1. The A_2 values are of order $10^{-4} \text{ cm}^3 \text{ mol g}^{-2}$, indicating that methanol at 25.0 °C is a good solvent for the present R samples as well as for the previous T and B samples.

Figure 4 shows double-logarithmic plots of A_2 (in $\text{cm}^3 \text{ mol g}^{-2}$) against M_w for PNIPA in methanol at 25.0 °C. For comparison, plots for the T and B samples have been reproduced from Figure 2 of ref. 2. The symbols and curves have the same meaning as those in Figure 3. The values of A_2 for the R samples are in rather good agreement with the values for the T samples over the whole range of M_w examined and are definitely larger than the values for the B samples. The quantity A_2 is proportional to an effective volume, excluded to a polymer chain by the presence of another, and decreases with an increasing degree of branching. Therefore, the above result indicates that the effective volume of a given R sample is almost the same as that of a T sample with the same M_w .

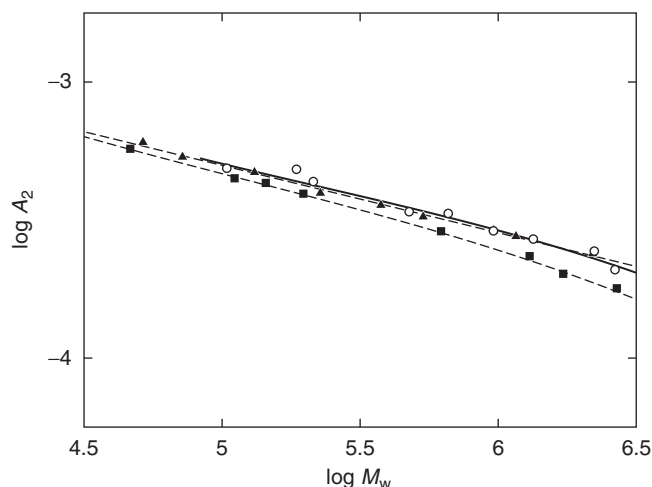


Figure 4 Double-logarithmic plots of A_2 (in $\text{cm}^3 \text{ mol g}^{-2}$) against M_w for poly(*N*-isopropylacrylamide) in methanol at 25.0 °C. The symbols and curves have the same meaning as those in Figure 3.

The seventh column of Table 1 gives the values of the interpenetration function Ψ for the eight samples R19 through R270 in methanol at 25.0 °C calculated from

$$\Psi = \frac{A_2 M_w^2}{4\pi^{3/2} N_A \langle S^2 \rangle^{3/2}} \quad (1)$$

with the values of M_w , $\langle S^2 \rangle$ and A_2 given in the third, fifth and sixth columns, respectively, of the table, where N_A is the Avogadro constant. The quantity Ψ , which is nearly equal to 0.24 for linear flexible polymers with very large M_w in good solvents, is sensitive to the density profile of repeat units constituting a given polymer^{14,15} and becomes larger than 0.24 if the segment density of the polymer is larger than that of the linear flexible polymers.

Figure 5 shows plots of Ψ against $\log M_w$ for the R samples in methanol at 25.0 °C along with plots for the T and B samples, which have been reproduced from Figure 4 of ref. 2. The unfilled circles, filled triangles, filled squares and solid and dashed curves have the same meaning as those in Figures 3 and 4. For comparison, literature data for linear PS (◆),^{16,17} regular 4-arm star PS (◈)¹⁸ and regular 6-arm star PS (◈),¹⁹ all measured in benzene at 25.0 °C, are also shown in Figure 5; the dotted curves smoothly connect the data points for each kind of PS. The value of Ψ for PS increases with the increasing number of arms because of the above-mentioned nature of Ψ . Note that the linear PS corresponds to two-arm star PS.

As a natural consequence of the behavior of $\langle S^2 \rangle$ and A_2 , shown in Figures 3 and 4, respectively, Ψ for the R samples is close to that for the T samples in the M_w range of $\lesssim 2 \times 10^6$, but deviates upward as M_w increases from $\sim 2 \times 10^6$. As for the B samples, Ψ increases with increasing M_w and becomes larger than Ψ for the regular four-arm star PS, which indicates that the degree of branching in the B samples is definitely larger than that in the R and T samples.

Intrinsic viscosity in methanol at 25 °C. The values of $[\eta]$ and k' determined from viscosity measurements in methanol at 25.0 °C for all nine samples, R10 through R270, are given in the eighth and ninth columns of Table 1. In accordance with the fact that methanol at 25.0 °C is also a good solvent for the present R samples as in the cases of the previous T and B samples, deduced from the above-mentioned results of A_2 , the k' values lie between 0.3 and 0.4.

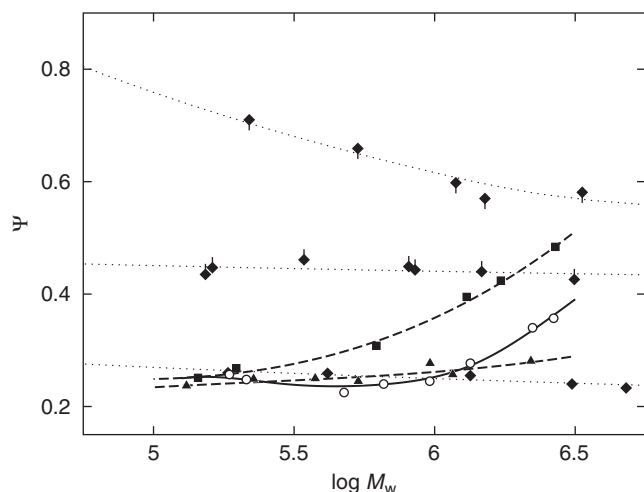


Figure 5 Plots of Ψ against $\log M_w$. The symbols \circ , \blacktriangle , \blacksquare and solid and dashed curves have the same meaning as those in Figure 3. The other symbols represent the literature data for polystyrene (PS) in benzene at 25.0 °C: (\blacklozenge) linear PS;^{16,17} (\blacklozenge) regular 4-arm star PS;¹⁸ (\blacklozenge) regular 6-arm star PS.¹⁹ The dotted curve smoothly connects the data points for each kind of PS.

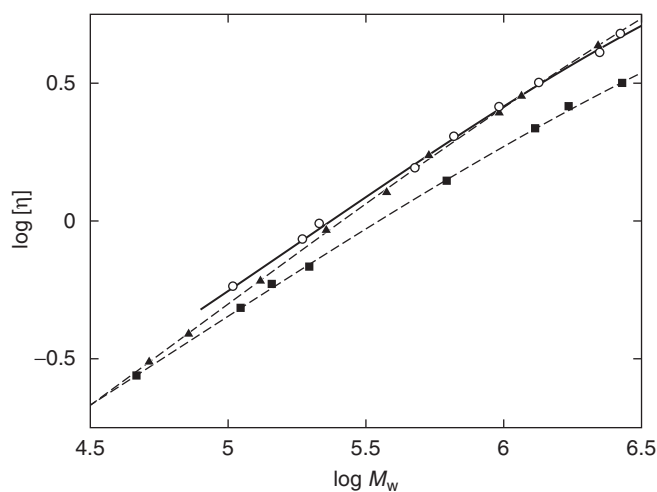


Figure 6 Double-logarithmic plots of $[\eta]$ (in 100 ml per g) against M_w for poly(*N*-isopropylacrylamide) in methanol at 25.0 °C. The symbols and curves have the same meaning as those in Figure 3.

Figure 6 shows double-logarithmic plots of $[\eta]$ (in 100 ml per g) against M_w for PNIPA in methanol at 25.0 °C. For comparison, plots for the T and B samples have been reproduced from Figure 3 of ref. 2. The symbols and curves have the same meaning as those in Figures 3 and 4. As in the cases of $\langle S^2 \rangle$ and A_2 , shown in Figures 3 and 4, respectively, the values of $[\eta]$ for the R samples are in rather good agreement with the values for the T samples and definitely larger than the values for the B samples. The quantity $[\eta]$ is proportional to the hydrodynamic (molar) volume and decreases with the increasing degree of branching. Therefore, the above result indicates that the hydrodynamic volume of a given R sample is almost the same as that of a T sample with the same M_w . The slope of the plot for the R samples in the range of $M_w \gtrsim 10^6$ is 0.5₈ and is smaller than 0.8, which corresponds to linear flexible polymers with very large M_w in good solvents, as in the cases of the T and B samples.² As a minor point, we note that the values of $[\eta]$ for the R samples with $M_w \lesssim 10^5$ are somewhat larger than the values for the T samples. This subtle discrepancy may arise from the

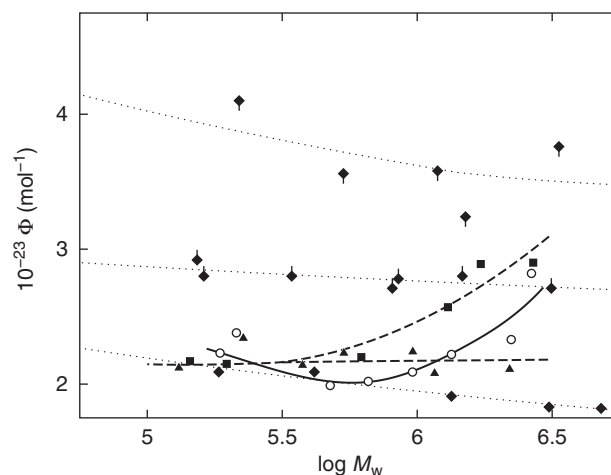


Figure 7 Plots of Φ (in mol^{-1}) against $\log M_w$. The symbols \circ , \blacktriangle , \blacksquare and solid and dashed curves have the same meaning as those in Figure 3. The other symbols \blacklozenge , \blacklozenge , \blacklozenge and the dotted curves have the same meaning as those in Figure 5.

difference in the effective hydrodynamic volume of the chain-end group between the R and T samples.

The last column of Table 1 gives the values of the Flory–Fox factor Φ for the eight samples, R19 through R270, in methanol at 25.0 °C calculated from

$$\Phi = \frac{M_w [\eta]}{6^{3/2} \langle S^2 \rangle^{3/2}} \quad (2)$$

with the values of M_w , $\langle S^2 \rangle$ and $[\eta]$ given in the third, fifth and eighth columns, respectively, of the table. The quantity Φ , which is nearly equal to $2 \times 10^{23} \text{ mol}^{-1}$ for linear flexible polymers with very large M_w in good solvents, is sensitive to the degree of branching of a given polymer and takes a larger value if the polymer has branches.

Figure 7 shows plots of Φ against $\log M_w$ for the R samples in methanol at 25.0 °C along with plots for the T and B samples, which have been reproduced from Figure 5 of ref. 2 and plots for the linear, regular 4-arm and regular 6-arm PS.^{16–19} All the symbols and curves have the same meaning as those in Figure 5. The difference in the behavior of Φ among the R, T and B samples is almost the same as in the case of Ψ shown in Figure 5.

From the results of the ^1H - and ^{13}C -NMR spectra and the dilute solution properties given in this subsection, it may be concluded that the R samples have almost the same stereochemical compositions as those of the T and B samples, the same degree of branching as that of the T samples for $M_w \lesssim 2 \times 10^6$, and the hydrophilic sulfonate group at the initiating end in place of the hydrophobic isobutyronitrile group for the T and B samples.

Cloud point in aqueous solutions

Figure 8 shows plots of the (relative) transmittance against temperature for the aqueous solutions of the PNIPA samples, R10 and R19, both at $w=5.05\%$. It should be noted here that the shape of the transmittance curve for each solution is almost independent of the rate of increase in temperature if the rate is slower than $1.5 \text{ }^\circ\text{C h}^{-1}$. For comparison, the transmittance curves (dashed) previously determined for the aqueous solutions of the T samples, T5 ($M_w=5.17 \times 10^4$) and T13 ($M_w=1.31 \times 10^5$), and the B samples, B5 ($M_w=4.65 \times 10^4$) and B14 ($M_w=1.44 \times 10^5$), all at $w \approx 5\%$, have been reproduced from Figure 2 of ref. 1. The curves for the R samples are located to the

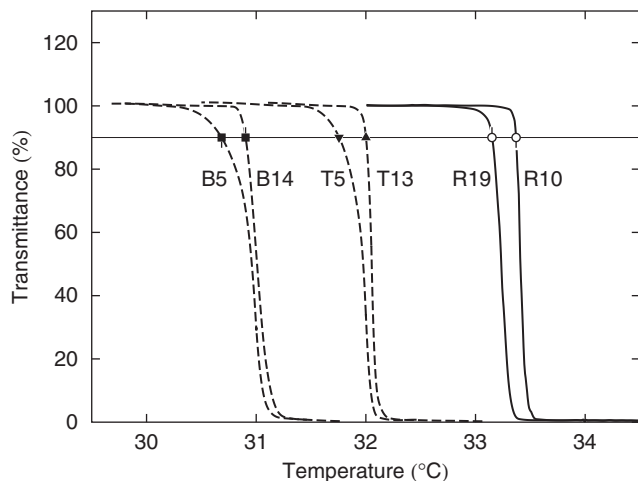


Figure 8 Temperature dependence of the transmittance of light passing through the aqueous solutions of the poly(*N*-isopropylacrylamide) (PNIPA) samples R10 and R19, both at $w=5.05\%$. The dashed curves represent the previous results for the aqueous solutions of the PNIPA samples T5, T13, B5 and B14, all at $w\approx 5\%$.¹ The horizontal line indicates the threshold value 90% and the symbol on each curve indicates the cloud point.

right (high temperature side) of the curves for the T and B samples. It is interesting to see that the curve moves to the right (high temperature side) with increasing M_w for the T and B samples, but moves to the left (low-temperature side) with increasing M_w for the R samples.

The cloud point in a given test solution is, in principle, determined to be the temperature at which the solution just starts to become turbid. As seen from Figure 8, however, it is somewhat difficult to determine such a temperature unambiguously because the transmittance for each solution starts to decrease from 100% rather gently. Following the previous studies,^{1,3} therefore, the cloud point in each solution was determined as the temperature at which the transmittance became the threshold value 90%, for convenience. In Figure 8, the symbols \circ and \odot represent the cloud points determined for samples R10 and R19, respectively, and the symbols ∇ , \blacktriangle , \blacksquare and \blacklozenge represent the cloud points previously¹ determined for samples T5, T13, B5 and B14, respectively. As a natural consequence of the behavior of the transmittance curves, the cloud points for the R samples are the highest among the three kinds of samples.

Finally, Figure 9 shows the cloud-point curves in aqueous solutions of the R samples R10 (\circ) and R19 (\odot) in the range of $0.5\% \lesssim w \lesssim 10\%$. For comparison, the cloud-point curves previously determined in aqueous solutions of the T samples T5 (∇) and T13 (\blacktriangle) and of the B samples B5 (\blacksquare) and B14 (\blacklozenge) have been reproduced from Figure 3 of ref. 1. The solid and dashed curves smoothly connect the cloud points for the R samples and the T and B samples, respectively. In the figure, the literature data reported by de Azevedo *et al.*²⁰ are also shown by the symbols \bullet . Although their PNIPA sample with $M_w=6.15 \times 10^5$ was prepared in the same manner as in the case of the present R samples, their experimental procedure to determine the cloud point was different from ours: the temperature at which the slope of the plot of the reciprocal of the intensity of light scattered from an aqueous PNIPA solution against temperature changes suddenly during the heating process was adopted as the cloud point. Despite the difference in M_w and the procedure to determine the cloud point, the present data for R10 and R19 qualitatively agree with the data by de Azevedo *et al.*²⁰

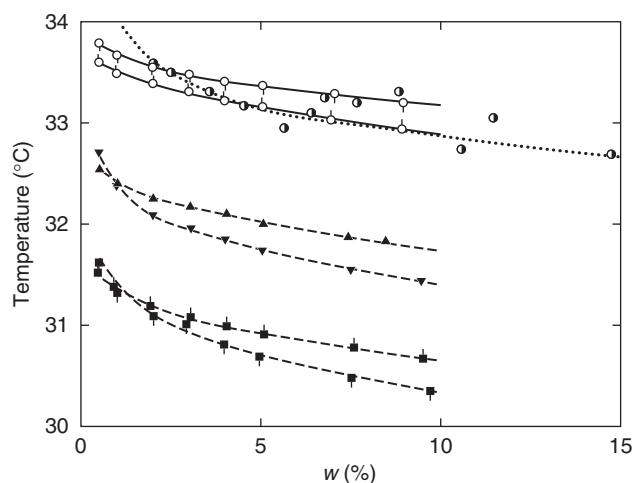


Figure 9 Cloud-point curves in aqueous solutions of poly(*N*-isopropylacrylamide): (\circ) R10; (\odot) R19; (∇) T5;¹ (\blacktriangle) T13;¹ (\blacksquare) B5;¹ (\blacklozenge) B14;¹ (\bullet) literature data for the sample with $M_w=6.15 \times 10^5$ by de Azevedo *et al.*²⁰ The curves smoothly connect the respective data points.

As expected from the results shown in Figure 8, the cloud-point curves for the R samples are located on the high temperature side among the three kinds of samples over the whole range of w examined. It is more important to note that the cloud-point curve for the R samples shifts to the low-temperature side with increasing M_w , while the curves for the T and B samples in the range of $w \gtrsim 2\%$ shift to the opposite side. Otake *et al.*²¹ and Schild and Tirrell⁶ pointed out that the cloud point in an aqueous solution of PNIPA synthesized by aqueous redox polymerization was somewhat higher than that of PNIPA synthesized by radical polymerization in organic solvents using AIBN as an initiator, although the reductive reagent *N,N,N',N'*-tetramethylethylenediamine of a redox catalyst used by them was different from ours. Furthermore, Xia *et al.*^{22,23} reported that the cloud point in an aqueous solution of PNIPA synthesized by atom transfer radical polymerization with a hydrophilic nonionic group at the initiating chain-end decreased with increasing molecular weight. These experimental results are consistent with ours, as shown in Figure 9. The dependence of the cloud point on M_w for the R samples is rather consistent with the prediction of conventional polymer solution thermodynamics.²⁴ We note that such dependence could also result from the hydrophilicity of the chain-end group: the hydrophilic effect increases with decreasing M_w .

It was previously³ shown that the cloud-point curve in an aqueous solution of a PNIPA sample with a strongly hydrophobic chain-end group, which was synthesized by living anionic polymerization and had the diphenylmethyl group at the initiating chain-end, shifted remarkably to the low-temperature side with decreasing M_w . Furthermore, it was recently reported that amphiphilic A-B block copolymers with a PNIPA block as the hydrophilic part formed aggregates in their aqueous solutions, and their cloud points were lower than those in an aqueous PNIPA solution.^{25–28} These facts imply that the above-mentioned noteworthy difference in the behavior of the cloud-point curve between the R sample and the T and B samples arises from the hydrophobicity of the chain-end groups, whose effect relatively increases with decreasing M_w .

We close our discussion with reference to the previous opinion about the difference in the behavior of the cloud points between the T

and B samples:^{1,2} the increase in the number of branch points results in the increase in the number of hydrophobic chain-end groups and, therefore, in the decrease in the cloud point.

CONCLUSION

The series of PNIPA samples having sulfonate groups at the initiating chain-ends were prepared by aqueous redox polymerization using a redox catalyst consisting of $(\text{NH}_4)_2\text{S}_2\text{O}_8$ and $\text{Na}_2\text{S}_2\text{O}_5$, which were referred to as R samples. The R samples were shown to have the same stereochemical compositions as those of the PNIPA samples, previously¹ synthesized by radical polymerization using AIBN as an initiator in *tert*-butanol and benzene, which were called T and B samples, respectively. From the analyses of $\langle S^2 \rangle$, A_2 and $[\eta]$ in methanol at 25.0 °C, the R samples were shown to have the same degree of branching as that of the T samples in the range of $M_w \lesssim 2 \times 10^6$, but have a somewhat larger degree of branching for $M_w \gtrsim 2 \times 10^6$ (the degree of branching of the B samples is the largest of all.²)

For the aqueous solutions of the two R samples, R10 ($M_w = 1.04 \times 10^5$) and R19 ($M_w = 1.86 \times 10^5$), the cloud-point curves were determined in the range of $0.5\% \lesssim w \lesssim 10\%$. The curves for R10 and R19 were appreciably higher than the curves previously¹ determined for the two T samples ($M_w = 5.17 \times 10^4$, $M_w = 1.31 \times 10^5$). (The curves for the B samples were lower than those for the T samples.¹) It was found that the cloud-point curve for the R samples shifts to the low-temperature side with increasing M_w , while the curves for the T and B samples in the range of $w \gtrsim 2\%$ shift to the opposite side. The difference in the behavior of the cloud-point curve between the R and T samples, both with almost the same degree of branching and stereochemical composition, arises from the difference in the chain-end group: the R samples have the hydrophilic sulfonate group and the T samples have the hydrophobic isobutyronitrile group.

ACKNOWLEDGEMENTS

This research was supported by a Grant-in-Aid (22350050) and in part by the global COE program International Center for Integrated Research and Advanced Education in Materials Science, from the Ministry of Education, Culture, Sports, Science and Technology, Japan.

- Kawaguchi, T., Kojima, Y., Osa, M. & Yoshizaki, T. Cloud points in aqueous poly(*N*-isopropylacrylamide) solutions. *Polym. J.* **40**, 455–459 (2008).
- Kawaguchi, T., Kojima, Y., Osa, M. & Yoshizaki, T. Primary structure of poly(*N*-isopropylacrylamide) synthesized by radical polymerization. Effects of polymerization solvents. *Polym. J.* **40**, 528–533 (2008).
- Kobayashi, K., Yamada, S., Nagaoka, K., Kawaguchi, T., Osa, M. & Yoshizaki, T. Characterization of linear poly(*N*-isopropylacrylamide) and cloud points in its aqueous solutions. *Polym. J.* **41**, 416–424 (2009).
- Kawaguchi, T., Kobayashi, K., Osa, M. & Yoshizaki, T. Is a 'cloud-point curve' in aqueous poly(*N*-isopropylacrylamide) solution binodal? *J. Phys. Chem. B* **113**, 5440–5447 (2009).
- Wooten, W. C., Blanton, R. B. & Coover, H. W. Effect of pH on homopolymerization of *N*-isopropylacrylamide. *J. Polym. Sci.* **25**, 403–412 (1957).
- Schild, H. G. & Tirrell, D. A. Microcalorimetric detection of lower critical solution temperatures in aqueous polymer solutions. *J. Phys. Chem.* **94**, 4352–4356 (1990).
- Deželić, G. & Vavra, J. Angular dependence of the light scattering in pure liquids. *Croat. Chem. Acta* **38**, 35–47 (1966).
- Berry, G. C. Thermodynamic and conformational properties of polystyrene. I. Light-scattering studies on dilute solutions of linear polystyrenes. *J. Chem. Phys.* **44**, 4550–4564 (1966).
- Johnson, B. L. & Smith, J. in *Light Scattering from Polymer Solutions* (ed. Huglin, M. B.) Ch 2 (Academic Press, London, 1972).
- Isobe, Y., Fujioka, D., Habaue, S. & Okamoto, Y. Efficient lewis acid-catalyzed stereocontrolled radical polymerization of acrylamides. *J. Am. Chem. Soc.* **123**, 7180–7181 (2001) and its supporting information.
- Zeng, F., Tong, Z. & Feng, H. N.m.r. investigation of phase separation in poly(*N*-isopropylacrylamide)/water solutions. *Polymer* **38**, 5539–5544 (1997).
- Ebdon, J. R., Huckerby, T. N. & Hunter, T. C. Free-radical aqueous slurry polymerizations of acrylonitrile: 1. End-groups and other minor structures in polyacrylonitriles initiated by ammonium persulfate/sodium metabisulfite. *Polymer* **35**, 250–256 (1994).
- Omidian, H., Zohuriaan-Mehr, M. J. & Bouhendi, H. Aqueous solution polymerization of neutralized acrylic acid using $\text{Na}_2\text{S}_2\text{O}_8/(\text{NH}_4)_2\text{S}_2\text{O}_8$ redox pair system under atmospheric conditions. *Int. J. Polym. Mater.* **52**, 307–321 (2003).
- Yamakawa, H. *Modern Theory of Polymer Solutions* (Harper & Row, New York, 1971) Its electronic edition is available on-line at the URL: <http://www.molsci.polym.kyoto-u.ac.jp/archives/redbook.pdf>.
- Yamakawa, H. *Helical Wormlike Chains in Polymer Solutions* (Springer, Berlin, 1997).
- Miyaki, Y., Einaga, Y. & Fujita, H. Excluded-volume effects in dilute polymer solutions. 7. Very high molecular weight polystyrene in benzene and cyclohexane. *Macromolecules* **11**, 1180–1186 (1978).
- Miyaki, Y. *Dilute Solutions of Polystyrene over a Very Wide Range of Molecular Weight* (Ph. D. Thesis, Osaka University, Osaka, 1981).
- Okumoto, M., Nakamura, Y., Norisuye, T. & Teramoto, A. Excluded-volume effects in star polymer solutions: four-arm star polystyrene in benzene. *Macromolecules* **31**, 1615–1620 (1998).
- Okumoto, M., Iwamoto, Y., Nakamura, Y. & Norisuye, T. Excluded-volume effects in star polymer solutions. Six-arm star polystyrene in benzene. *Polym. J.* **32**, 422–427 (2000).
- de Azevedo, R. G., Rebelo, L. P. N., Ramos, A. M., Szydłowski, J., de Sousa, H. C. & Klein, J. Phase behavior of (polyacrylamides + water) solutions: concentration, pressure and isotope effects. *Fluid Phase Equilib.* **185**, 189–198 (2001).
- Otake, K., Inomata, H., Konno, M. & Saito, S. Thermal analysis of the volume phase transition with *N*-isopropylacrylamide gels. *Macromolecules* **23**, 283–289 (1990).
- Xia, Y., Yin, X., Burke, N. A. D. & Stöver, H. D. H. Thermal response of narrow-disperse poly(*N*-isopropylacrylamide) prepared by atom transfer radical polymerization. *Macromolecules* **38**, 5937–5943 (2005).
- Xia, Y., Burke, N. A. D. & Stöver, H. D. H. End group effect on the thermal response of narrow-disperse poly(*N*-isopropylacrylamide) prepared by atom transfer radical polymerization. *Macromolecules* **39**, 2275–2283 (2006).
- Flory, P. J. *Principles of Polymer Chemistry* (Cornell University Press, Ithaca, NY, 1953).
- Chung, J. E., Yokoyama, M., Suzuki, K., Aoyagi, T., Sakurai, Y. & Okano, T. Reversibly thermo-responsive alkyl-terminated poly(*N*-isopropylacrylamide) core-shell micellar structures. *Colloids Surf. B* **9**, 37–48 (1997).
- Chung, J. E., Yokoyama, M., Aoyagi, T., Sakurai, Y. & Okano, T. Effect of molecular architecture of hydrophobically modified poly(*N*-isopropylacrylamide) on the formation of thermoresponsive core-shell micellar drug carriers. *J. Control. Release* **53**, 119–130 (1998).
- Kujawa, P., Segui, F., Shaban, S., Diab, C., Okada, Y., Tanaka, F. & Winnik, F. M. Impact of end-group association and main-chain hydration on the thermosensitive properties of hydrophobically modified telechelic poly(*N*-isopropylacrylamides) in water. *Macromolecules* **39**, 341–348 (2006).
- Duan, Q., Narumi, A., Miura, Y., Shen, X., Sato, S., Satoh, T. & Kakuchi, T. Thermo-responsive property controlled by end-functionalization of poly(*N*-isopropylacrylamide) with phenyl, biphenyl, and triphenyl groups. *Polym. J.* **38**, 306–310 (2006).